Nutlin-3a Activates p53 to Both Down-regulate Inhibitor of Growth 2 and Up-regulate *mir-34a, mir-34b,* and *mir-34c* Expression, and Induce Senescence

Kensuke Kumamoto,[1,4] Elisa A. Spillare,[1] Kaori Fujita,[1] Izumi Horikawa,[1] Taro Yamashita,[1] Ettore Appella,[2] Makoto Nagashima,[3] Seiichi Takenoshita,[4] Jun Yokota,[5] and Curtis C. Harris[1]

[1]Laboratory of Human Carcinogenesis and [2]Laboratory of Cell Biology, Center for Cancer Research, National Cancer Institute, NIH, Bethesda, Maryland; [3]Department of Surgery, Toho University Sakura Hospital, Sakura, Japan; [4]Second Department of Surgery, Fukushima Medical University School of Medicine, Fukushima, Japan; and [5]Biology Division, National Cancer Center Research Institute, Tokyo, Japan

Abstract

Nutlin-3, an MDM2 inhibitor, activates p53, resulting in several types of cancer cells undergoing apoptosis. Although p53 is mutated or deleted in ~50% of all cancers, p53 is still functionally active in the other 50%. Consequently, nutlin-3 and similar drugs could be candidates for neoadjuvant therapy in cancers with a functional p53. Cellular senescence is also a phenotype induced by p53 activation and plays a critical role in protecting against tumor development. In this report, we found that nutlin-3a can induce senescence in normal human fibroblasts. Nutlin-3a activated and repressed a large number of p53-dependent genes, including those encoding microRNAs. *mir-34a, mir-34b*, and *mir-34c*, which have recently been shown to be downstream effectors of p53-mediated senescence, were up-regulated, and inhibitor of growth 2 (*ING2*) expression was suppressed by nutlin-3a treatment. Two candidates for a p53-DNA binding consensus sequence were found in the *ING2* promoter regulatory region; thus, we performed chromatin immunoprecipitation and electrophoretic mobility shift assays and confirmed p53 binding directly to those sites. In addition, the luciferase activity of a construct containing the ING2 regulatory region was repressed after p53 activation. Antisense knockdown of *ING2* induces p53-independent senescence, whereas overexpression of *ING2* induces p53-dependent senescence. Taken together, we conclude that nutlin-3a induces senescence through p53 activation in normal human fibroblasts, and p53-mediated *mir34a, mir34b*, and *mir34c* up-regulation and ING2 down-regulation may be involved in the senescence pathway. [Cancer Res 2008;68(9):3193–203]

Introduction

p53 has many functions in its role as a tumor suppressor gene (1). It is well-documented that *p53* is a critical mediator of the senescence response to several stimuli, such as DNA damage, oncogene activation, oxidative stress, and overexpression of tumor suppressor genes (2, 3). Cellular senescence is mainly classified into two types based on the mechanism. One is replicative senescence, which is involved with telomere-shortening and found in human fibroblast strains (4). The other is telomere-independent cellular senescence, called premature senescence and is induced by cellular stress. p53 plays a pivotal role for both types of cellular senescence. Recent reports show that the senescence response by p53 activation is considered to be one of the mechanisms protecting against malignant transformation (5, 6).

Under normal physiologic conditions, p53 expression is maintained at low levels in proliferating cells by degradation via MDM2 functioning as an E3 ubiquitin ligase (7). MDM2 is overexpressed in several human cancers, especially in sarcomas (8). ADP ribosylation factor (ARF) functions in part to activate p53 through MDM2 inhibition (9, 10). Because MDM2 inhibition could be effective for p53 stabilization and accumulation, several MDM2 inhibitors have been recently developed for potential cancer therapy (11). Nutlin-3, which is one of the MDM2 inhibitors, is a small molecule that binds to MDM2 so that it functions as an activator of p53 expression due to the interference of binding between p53 and MDM2 (11–13). Recent reports have shown that nutlin-3 induces p53-dependent apoptosis and cell cycle arrest in several kinds of cancer cell lines that contain wild-type p53 (14, 15). The effect was especially dramatic in cancer cells that overexpress MDM2, such as certain sarcomas. Although phosphorylation of various serine resides on p53 NH_2 terminal domain was not detected after nutlin-3 treatment, p53 seems to be fully active as a transcription factor and apoptotic inducer (16). Moreover, nutlin-3 also prevented the association of MDM2 with both hypoxia-inducible factor 1α, so that the induction of vascular endothelial growth factor was attenuated (17), and E2F1, which allowed transcriptional activation of *p73α* and *NOXA* resulting in apoptosis (18). Nutlin-3 has the potential to perform various functions through MDM2 inhibition. In the present study, our initial aim was to investigate if nutlin-3 induced senescence in normal human fibroblasts.

When *p53* is activated by several stimuli, many genes are regulated positively and negatively. Previous reports have examined changes in p53-related genes after different treatments that activate *p53* (19–21). Although p53 induces cellular senescence, the mRNA expression pattern exhibited some differences between replicative senescence and premature senescence (22, 23). In addition to p53-related mRNA expression, recent reports have shown that microRNA-34s (*mir-34a, mir-34b*, and *mir-34c*) are downstream effectors of p53-dependent senescent and apoptotic pathways (24–27).

In this study, we further focused on the inhibitor of growth 2 (*ING2*) gene, a potential nutlin-3–induced *p53*-responsive gene, which was down-regulated by the treatment of nutlin-3 in the microarray experiments. *ING2* is a member of the *ING* gene family, which contains a plant homeodomain finger (28). *ING2* may be a tumor suppressor gene associated with *p53* (29). Recent reports have
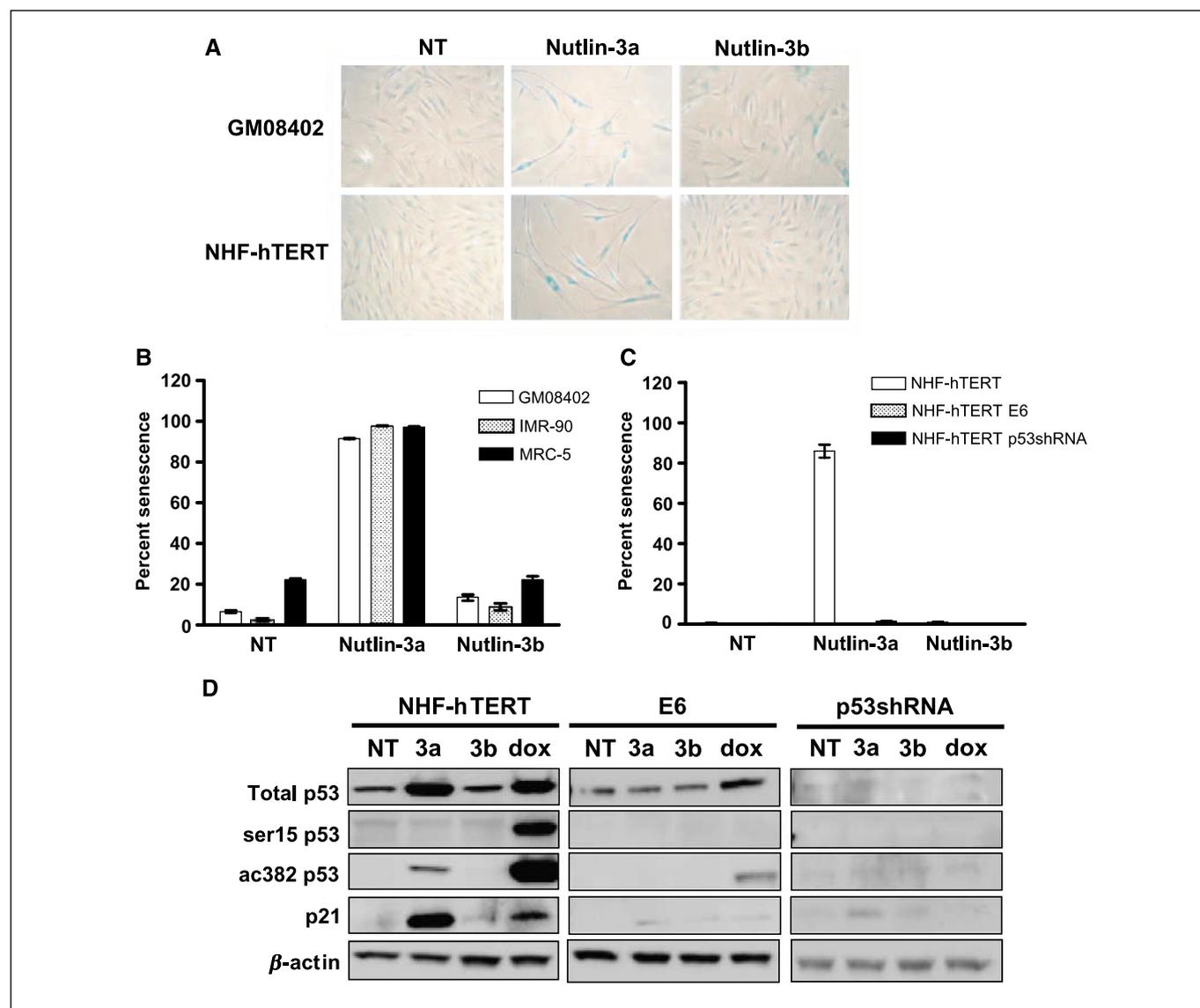
Figure 1. Nutlin-3a induces primary and immortalized normal human fibroblasts to undergo senescence in a p53-dependent manner. *A,* normal human fibroblasts, GM08402, and NHF-hTERT were treated with 10 μmol/L nutlin-3a, nutlin-3b, or left untreated (*NT*) for 7 d. SA-β-gal assay was performed after the treatment. Magnification, 200×. *B,* three primary fibroblast strains, GM08402, IMR-90, and MRC-5, were treated with 10 μmol/L nutlin-3a, nutlin-3b, or left untreated for 7 d. The percentage of cells stained by SA-β-gal was calculated. *Columns,* average of five random fields per dish of three independent experiments; *bar,* SD. *C,* NHF-hTERT, an E6-expressing cell line (NHF-hTERT E6), and a p53 shRNA-expressing cell line (NHF-hTERT p53 shRNA) were treated with 10 μmol/L nutlin-3a, nutlin-3b, or left untreated for 7 d. SA-β-gal was assayed after the treatment. *Columns,* as above; *bars,* SD. *D,* NHF-hTERT, NHF-TERT E6 (E6), and NHF-hTERT p53 shRNA (p53 shRNA) cells were treated with 10 μmol/L nutlin-3a (*3a*), nutlin-3b (*3b*), or left untreated for 24 h. As a positive control, each cell line was treated with 1 μmol/L doxorubicin (*dox*) for 24 h. Cell lysates from these cells were immunoblotted with the indicated antibodies.

shown that ING2 forms complexes with mSin3a and histone deacetylase 1 (HDAC1; ref. 30) and binds to the histone H3 trimethylated at lysine 4 (H3K4me3; refs. 31–33). This evidence indicates that ING2 is involved in chromatin remodeling to regulate gene activation or suppression. Specifically, it has been reported that H3K4me3 is associated with gene activation (34, 35). Chromatin structure consists of many forms of modification that regulate gene transcription; thus, the impairment of these epigenetic events may affect tumor development, cell proliferation, and senescence (36).

Materials and Methods

Cell culture. GM08402 primary human fibroblasts were obtained from the Coriell Cell Repositories. The hTERT-immortalized fibroblast cell line NHF-hTERT and the E6-expressing version of this cell line NHF-hTERT E6 were derived by infecting the primary cell strain GM07532 (Coriell Cell Repositories), as previously published (37). The NHF-hTERT p53 short hairpin RNA (shRNA) cell line was derived by transfecting p53 shRNA into the NHF-hTERT cells. Cultured human cancer cell lines, including RKO, LS174T, SW620, WiDr, A549, NCI-H157, NCI-H1299, Calu-6, MCF7, and U-2OS, as well as the primary fibroblasts, IMR-90, MRC-5, and WI-38, were originally obtained from American Type Culture Collection. MDAH 041 p53$^{-/-}$ were derived from fibroblasts of a patient with Li-Fraumeni syndrome and were kindly provided by Michael Tainsky (Case Western Reserve University). The HCT116 human colon cancer cell lines (p53$^{+/+}$ and p53$^{-/-}$) were kindly provided by Dr. Bert Vogelstein (Johns Hopkins University School of Medicine). All cells were grown at 37°C in the presence of 5% CO_2 in the recommended media.

Table 1. Nutlin-3a–induced p53-responsive genes in NHF-hTERT cells

Gene symbol	Genbank accession number	Mean of ratios in NHF-hTERT	Mean of ratios in NHF-hTERT shp53	Fold difference of means	Parametric *P* value
A. Up-regulated genes					
MDM2	NM_006879	23.051	1.203	19.161	<1e−07
BTG2	NM_006763	7.677	0.502	15.293	4.00e−07
TP53I3	NM_004881	7.227	1.476	4.896	1.00e−06
SULF2	NM_018837	17.253	1.075	16.049	1.30e−06
GDF15	NM_004864	13.951	1.206	11.568	1.60e−06
CYFIP2	NM_030778	4.682	0.88	5.32	2.30e−06
NINJ1	NM_004148	4.122	0.937	4.399	2.90e−06
LOC728364	XR_015271	2.78	0.578	4.81	3.20e−06
PLTP	NM_006227	12.503	1.059	11.806	4.70e−06
SESN1	NM_014454	4.912	0.772	6.363	1.02e−05
B. Down-regulated genes					
CCNB1	NM_031966	0.071	1.25	0.057	<1e−07
CENPF	NM_016343	0.05	0.885	0.056	<1e−07
CCNA2	NM_001237	0.09	0.889	0.101	<1e−07
CDKN3	NM_005192	0.079	0.972	0.081	<1e−07
SPAG5	NM_006461	0.063	1.005	0.063	1.00e−07
CKS2	NM_001827	0.104	1.05	0.099	1.00e−07
CASC5	NM_144508	0.067	0.988	0.068	1.00e−07
KIFC1	NM_002263	0.075	0.948	0.079	2.00e−07
CDC20	NM_001255	0.046	2.061	0.022	2.00e−07
KIF2C	NM_006845	0.086	0.952	0.09	2.00e−07

Drug treatment and senescence-associated β-galactosidase assays. Nutlin-3a and its enantiomer, nutlin-3b, were generous gifts from Dr. Lyubomir Vassilev (Hoffmann-La Roche, Inc.). Cells were plated at varying cell densities in either six-well dishes or 100 mm² dishes. Nutlin-3a or nutlin-3b was added at varying concentrations (0–10 μmol/L) after 24 h. Cells were then fixed in 2% formaldehyde/0.2% glutaraldehyde in PBS for 5 min and incubated at 37°C for 12 to 18 h with fresh senescence-associated β-galactosidase (SA-β-gal) stain solution containing 1.0 mg/mL X-gal (37). Doxorubicin and trichostatin A (Sigma-Aldrich) were used at the indicated concentrations.

Immunoprecipitation and Western blotting. Protein lysates were prepared as described previously (19). p53 immunoprecipitation was done by incubating with agarose-conjugated DO-1 and Pab 1801 (Santa Cruz) antibodies for 2 h. Proteins were electrophoresed on SDS-PAGE gels and transferred to Immobilon-P membrane (Millipore). Protein detection was done by using the following antibodies: p53 (DO-1; Oncogene Science), ser15 p53 and ac382 p53 (Cell Signaling), threonine 18 p53 (gift from Dr. Ettore Appella), p21 (Oncogene Science), β-actin (Sigma), and rabbit polyclonal anti-ING2, which was generated against the COOH terminal 14mer amino acid of ING2. Bound antibodies were detected using enhanced chemiluminescence (ECL) detection reagents (Amersham Pharmacia Biotech) and visualized by autoradiography.

Microarray analysis. Microarray experiments were performed as previously described (19). Samples for the microarray experiments were prepared as follows: both NHF-hTERT and NHF-hTERT p53 shRNA cells were treated with 10 μmol/L nutlin-3a or the same amount of DMSO. Cells were harvested at 24 and 36 h after the treatment. The data analysis was performed using the BRB Array Tools.[6]

Real-time reverse transcription–PCR analysis of microRNA and mRNA expression. Total RNA from each cell line was harvested using TRIzol (Invitrogen) according to the manufacturer's protocol. For detecting

microRNA expression, reverse reactions were performed using TaqMan MicroRNA Assay kit (Applied Biosystems). Five micrograms of total RNA were used for the synthesis of first-strand cDNA using the SuperScript III First Strand cDNA Synthesis kit (Invitrogen) following the manufacturer's instructions. Real-time PCR analysis was performed using ABI prism 7500 (Applied Biosystems) with a TaqMan probe provided by the manufacturer. The TaqMan probes used were *ING2* (Id Hs00357543_m1), p21 (Id Hs00355782_m1), glyceraldehyde-3-phosphate dehydrogenase (GAPDH; Id Hs99999905_m1), hsa-mir-34a, hsa-mir-34b, hsa-mir-34c, and RNU66. The relative amounts of the mRNA and microRNA targeted gene were normalized by the amount of *GAPDH* and *RNU66* transcript, respectively.

Chromatin immunoprecipitation. Chromatin immunoprecipitation (ChIP) was performed using the ChIP Assay kit (Upstate) according to the manufacturer's protocol. PCR reactions contained 4 μL of immunoprecipitate or diluted total input, 500 nmol/L of each primer, 200 nmol/L deoxynucleotide triphosphate, 500 nmol/L MgSO₄, and 1 unit KOD plus (Toyobo) in a total volume of 50 μL. The primers for detecting the expected p53 DNA binding sequence were designed as follows: *ING2* site 1, forward 5′-AGATTCCAGCGTAGGGGAAG-3′ and reverse 5′-CTTTTCGGACGACCTG-GAG-3′; *ING2* site 2, forward 5′-AGGCTAGCGGGAGGCTCT-3′ and reverse 5′-CTCCAGGACCGGAGCAGT-3′. After 32 to 35 cycles of amplification, PCR products were run on a 1.5% agarose gel and analyzed by ethidium bromide staining.

Electrophoretic mobility shift analysis. Electrophoretic mobility shift assays (EMSA) were carried out using the LightShift Chemiluminescent EMSA kit (Pierce). The oligonucleotide with the p53 binding site, from −890 to −851 of the *ING2* promoter, called *ING2* site 1, was 5′-TCCCTGATCAT-CAGCCCCGCGGTGCCGGGCGAGCCCGAGGGC-3. Another oligonucleotide with the *p53* binding site of the *ING2* promoter (from −268 to −229), named *ING2* site 2, was 5′-GACTGGGGACAGGCGGGCGGCGACGGGCTTG-TCATGGGGA-3. All oligonucleotides were hybridized with complementary-synthesized oligonucleotides and used in double-stranded form. The oligonucleotides were labeled with biotin. The DNA binding reaction of biotinated double-stranded oligonucleotides with 10 ng of recombinant

---

[6] http://linus.nci.nih.gov/BRB-ArrayTools.html
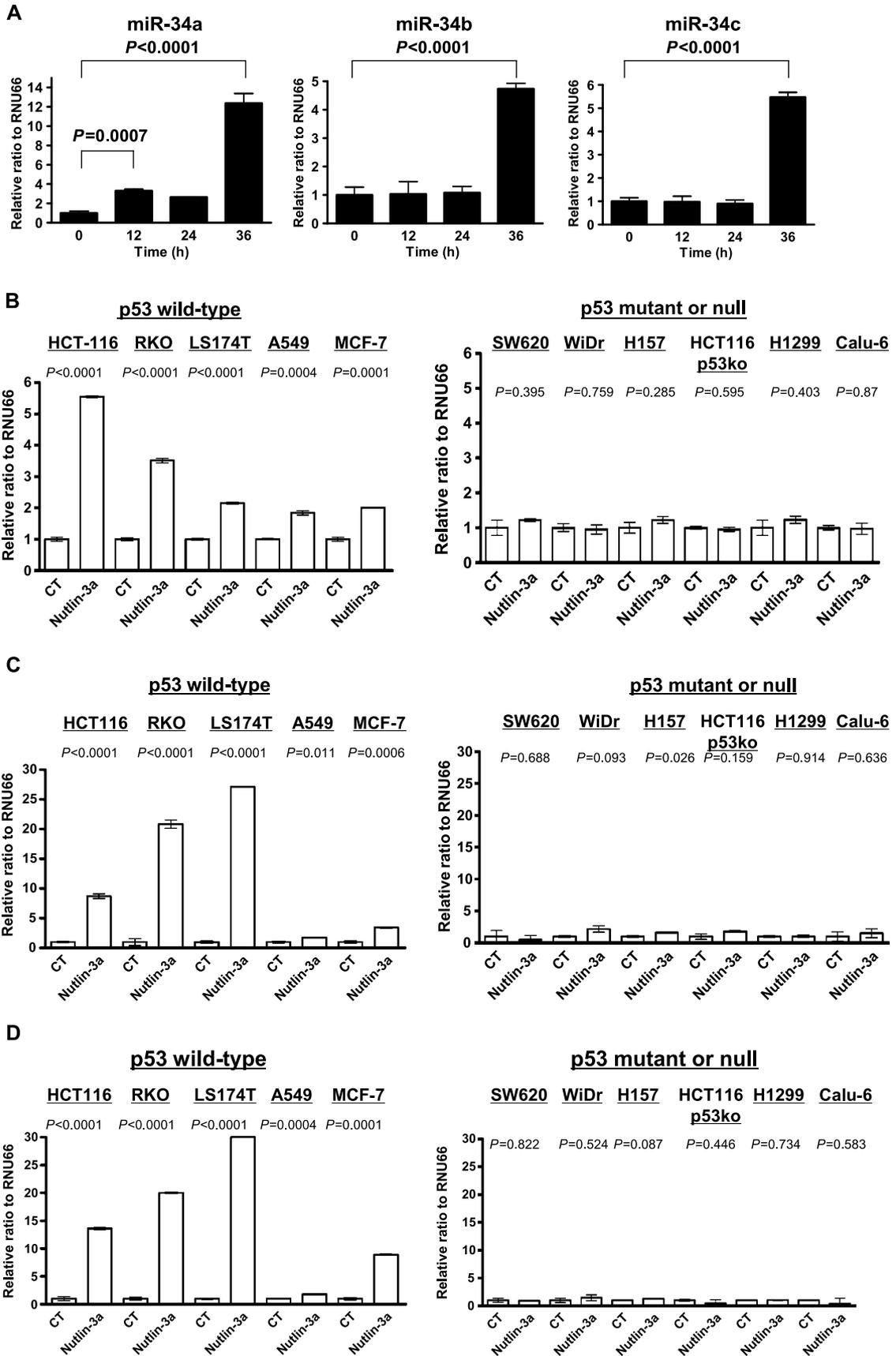
p53 (active motif) was done at room temperature for 20 min according to the manufacturer's protocol in $1\times$ binding buffer, containing 2.5% glycerol, 5 mmol/L $MgCl_2$, 0.05% NP40, and 50 ng/μL poly(deoxyadenylate-deoxyTMP). Anti-p53 (DO-1) antibody and anti-Sp1 antibody (Santa Cruz) were used for detecting a super-shifted band. Unlabeled oligonucleotides were used as competitors. DNA-protein complexes were detected by the ECL method.

Luciferase assay. The reporter construct for *ING2*(A) containing −1251 to +140 bases from the putative transcription start site and *ING2*(C) containing −413 to +140 bases from the putative transcription start site were prepared by PCR amplification from the human genomic DNA of Beas2B, a normal human lung epithelial cell line. The products were cloned into the *Mlu*I and *Bgl*II sites of the pGL-3 basic vector (Promega). The construct for *ING2*(B) was generated from the *ING2*(A) by digesting the region from −560 to −162 using *sma*I. The construct for *ING2*(D) containing −162 to +140 bases was further modified from the *ING2*(B).

A dual-luciferase assay was performed in triplicate according to the manufacturer's instructions (Promega). 1×10^5 cells were plated on 12-well plates 1 d before transfection. A pGL-3 luciferase reporter (1.6 μg) and 0.16 μg of the *Renilla* luciferase assay vector pRL (Promega) were cotransfected into HCT116 and RKO cells using Lipofectamine 2000 (Invitrogen) according to the manufacturer's protocol. At 24 h posttransfection, the cells were treated with nutlin-3a or were left untreated. Cell lysates were obtained by adding 250 μL of cell lysis buffer per well. Luciferase activity was measured by using 20 μL of cell lysate per assay tube in a single-photon channel of a scintillation counter (Beckman). The level of firefly luciferase activity was normalized by that of the *Renilla* luciferase activity in each experiment.

Small interfering RNA, overexpression, and antisense experiments. The *ING-2* small interfering RNAs (siRNA; Invitrogen) were designed as follows: ING2-1, 5-ACACAAAUGCUCGAAUUGGUGGAAA-3′ and ING2-2, 5′-ACAUACUGCUUAUGCAACCAAGUGU-3′. The scrambled siRNA sequences were 5-ACAAAGUUCGCAAUUGGGGUGACAAA-3. These were transfected into the NHF-hTERT cells using the Lipofectamine 2000 reagent (Invitrogen) according to the manufacturer's protocol. For Western blotting, cells were treated 24 h with nutlin-3a, nutlin-3b, or no treatment at 72 h posttransfection. For the SA-β-gal assay, cells were treated with the nutlins or left untreated for 3 d at 24 h posttransfection. The *ING2* complete cDNA expression vector was transferred into an adenovirus-packing cell line. The high-titer purified preparations were generated by Gene Expression Laboratory of National Cancer Institute-Frederick. GFP gene expression in IMR-90, MRC-5, and WI-38 cells treated with the GFP inserted adenovirus (adeno-GFP) at a multiplicity of infection (MOI) of 100 was observed in ~90% of the cells. The cells were treated with 100 MOI adeno-*GFP* or *ING2* inserted adenovirus (adeno-ING2) for 72 h. MSCV retroviral vectors encoded for *mir-34a* were kindly provided by Dr. Gregory L. Hannon (Watson School of Biological Sciences, Cold Spring Harbor Laboratory).

Results

Nutlin-3a induced cellular senescence in normal human fibroblasts. The normal human skin fibroblast strain GM08402 and the hTERT immortalized cell line NHF-hTERT were treated with nutlin-3a for 7 days. Nutlin-3b, which has a 150-fold lower affinity to MDM2 (13), was used as a negative control. After the treatment, the cells were fixed and stained for the low pH SA-β-gal activity (Fig. 1*A*). A high percentage of cells that had been treated with nutlin-3a were stained positive for the low pH β-gal, indicating cells had undergone senescence. Nutlin-3b–treated cells exhibited similar levels as the nontreated cells. Next, we determined the time and dose dependency of nutlin-3 in NHF-hTERT cells. In the time course, 50% of the cells were SA-β-gal positive at 3 days and almost 100% showed positive staining at 7 days after nutlin-3a treatment, whereas few positive cells were detected by treatment with nutlin-3b (Supplementary Fig. S1*A*). Cells were also treated with indicated concentrations of nutlin-3 for 7 days. Ninety percent of the cells were stained with SA-β-gal at 3 μmol/L nutlin-3a, whereas 1 μmol/L nutlin-3a showed a weak effect. All of the cells showed positive staining at 10 μmol/L, the reported maximal dose without toxicity (Supplementary Fig. S1*B*).

We further examined the effect of nutlin-3 treatment for other normal human lung fibroblast strains, IMR-90, MRC-5, and GM08402, and analyzed the number of positive cells by SA-β-gal staining. All three cell strains showed a morphologically senescent phenotype after nutlin-3a treatment. Again, almost 100% of the cells showed positive staining (Fig. 1*B*). There is a low percentage of β-gal–positive cells after nutlin-3b treatment; however, it was not a significant change compared with the untreated cells.

The hallmark of cellular senescence is an essentially irreversible arrest of cell division. To determine if the nutlin-induced senescence was reversible, colony-forming efficiencies (CFE) and population doublings (PD) were determined for cells after removal of the nutlin drugs. CFEs were determined by allowing the cells to be grown in the presence of 10 μmol/L nutlin-3a or nutlin-3b or left untreated for 7 days at subconfluence. Cells were then trypsinized, washed, and replated at densities of either 1×10^2 or 1×10^3 per 100 mm^2 dish in normal growth media for an additional 7 days. The cells were fixed and stained with crystal violet, and the number of colonies was counted. At both densities, the nutlin-3a–treated cells were unable to form a significant number of colonies compared with the untreated or nutlin-3b–treated cells. There was a 10-fold difference in the number of colonies formed (Supplementary Fig. S2*A*).

Next, we calculated the PDs for these cells after the same protocol as above, except that cells were plated at densities of either 1×10^3 or 1×10^4 per dish. Cells were trypsinized after 7 days and counted to determine population doublings. Results showed the nutlin-3a–treated cells could not divide after being replated because there was <0.1 PDs for either density (Supplementary Fig. S2*B*). On the other hand, the nutlin-3b or untreated cells underwent over 2.5 PDs, depending on the number of cells plated. Assuming that ~90% of the nutlin-3a–treated cells underwent senescence, these data support the hypothesis that

Figure 2. mir-34 expression was increased by nutlin-3a treatment in a p53-dependent manner. *A,* NHF-hTERT cells were treated with 10 μmol/L nutlin-3a for indicated time points. Total RNA (10 ng) extracted from each of the treated cells was used for real-time reverse transcription–PCR (RT-PCR) analysis of mir-34a, mir-34b, and mir-34c and RNU66 expression. RNU66 transcripts were used as an internal control. Statistical analysis was performed by Student's *t* test. *Columns,* average of three independent experiments; *bars,* SD. *B,* the human tumor cell lines shown were left untreated or treated with 10 μmol/L nutlin-3a for 24 h. Total RNA (10 ng) was then extracted and used for real-time RT-PCR analysis of mir-34a and RNU66 expression. RNU66 transcripts were used as an internal control. Statistical analysis was performed by Student's *t* test. *Columns,* average of three independent experiments; *bars,* SD. *C,* total RNA (10 ng) was then extracted from the same cell lines as above and used for real-time RT-PCR analysis of mir-34b and RNU66 expression. RNU66 transcripts were used as an internal control. Statistical analysis was performed by Student's *t* test. *Columns,* average of three independent experiments; *bars,* SD. *D,* the human tumor cell lines were left untreated or treated with 10 μmol/L nutlin-3a for 24 h. Total RNA (10 ng) was then extracted from the cells and used for real-time RT-PCR analysis of mir-34c and RNU66 expression. RNU66 transcripts were used as an internal control. Statistical analysis was performed by Student's *t* test. *Columns,* average of three independent experiments; *bars,* SD.
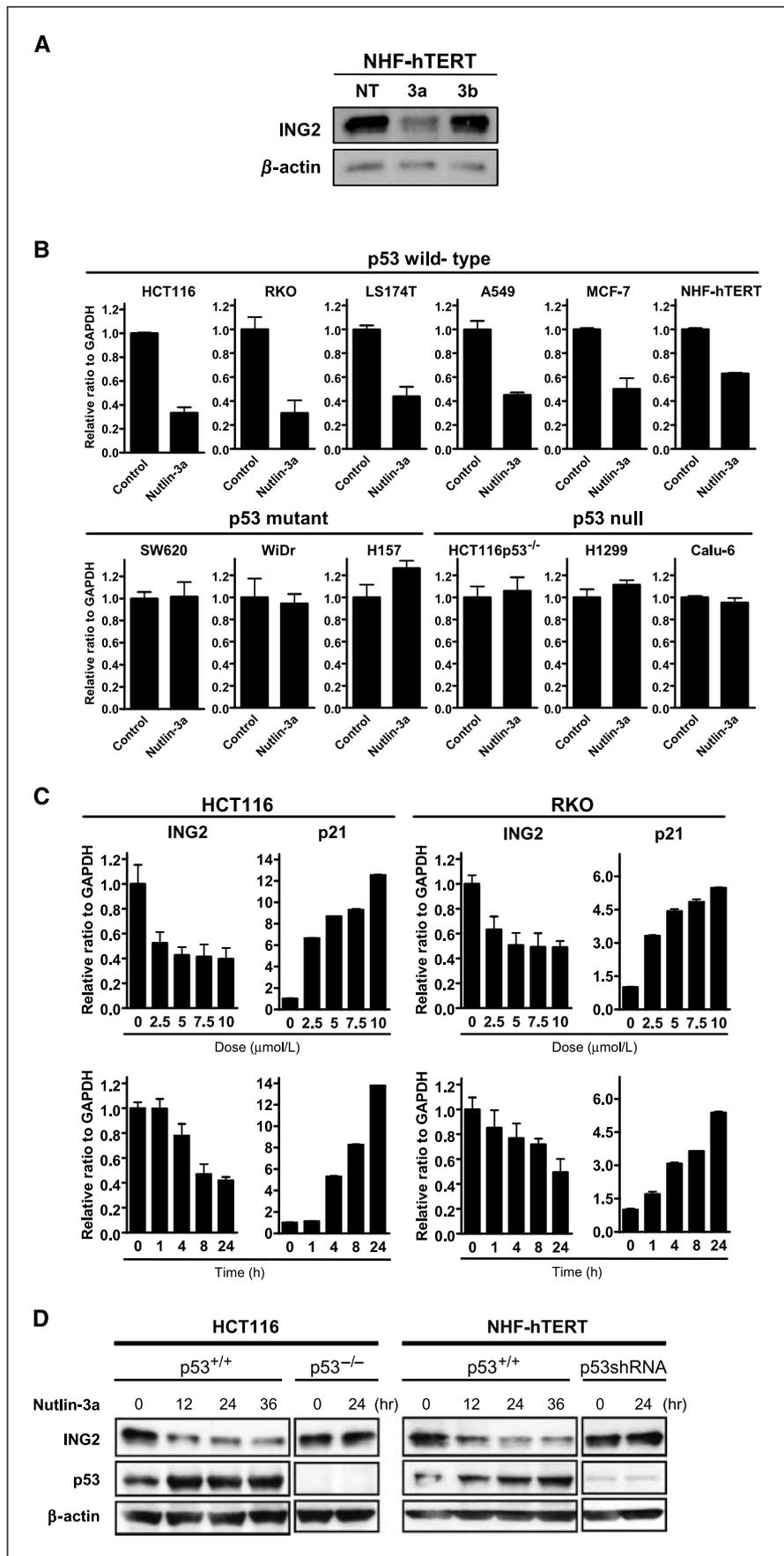
Figure 3. *ING2* expression was decreased by nutlin-3a treatment in a p53-dependent manner. *A,* NHF-hTERT cells treated with 10 μmol/L nutlin-3a, nutlin-3b, or untreated for 24 h were lysed for Western blot analysis of ING2 proteins. *B,* p53 wild-type cells (HCT116, RKO, LS174T, A549, MCF-7, and NHF-hTERT), p53 mutant cells (SW620, WiDr, and H157), and p53 null cells (HCT116 p53$^{-/-}$, H1299, and Calu-6) were treated with 10 μmol/L nutlin-3a for 24 h. The same amount of DMSO was added as a control. Total RNA extracted from each of the treated cells was used for real-time RT-PCR analysis of *ING2* and *GAPDH* mRNA expression. *GAPDH* mRNA transcripts were used as an internal control. *Columns,* average of three independent experiments; *bars,* SD. *C, top,* HCT116 p53$^{+/+}$ and RKO cells were treated with varying doses of nutlin-3a (0, 2.5, 5, 7.5, and 10 μmol/L) for 24 h. *Bottom,* HCT116 p53$^{+/+}$ and RKO cells were treated with 10 μmol/L nutlin-3a or the same amount of DMSO for indicated time points (0, 1, 4, 8, and 24 h). *ING2* and *p21* mRNA transcripts were measured by real-time RT-PCR analysis using indicated samples. These expressions were normalized by *GAPDH* mRNA expression. *Columns,* average of three independent experiments; *bars,* SD. *D,* the p53 isogenic pairs of HCT116 and NHF-hTERT were treated with 10 μmol/L nutlin-3a for indicated time points. The expression of ING2 was determined by Western blot analysis using total cell lysates prepared from these cells. β-Actin was probed as an internal control.

these nutlin-3a–treated cells have undergone a permanent senescence.

Nutlin-3a–induced senescence is dependent on p53. To determine if the senescence is induced in a p53-dependent manner,

p53-deficient cell lines, NHF-hTERT E6 and NHF-hTERT p53 shRNA, were exposed to nutlin-3a or nutlin-3b for 7 days. The parental cells, NHF-hTERT cells, exhibited the senescent phenotype after treatment with nutlin-3a, with over 80% of the cells stained by

Figure 4. p53 binds to *ING2* regulatory region and suppresses luciferase activity. *A,* HCT116 p53$^{+/+}$, HCT116 p53$^{-/-}$, NHF-hTERT, NHF-hTERT E6, and RKO cells were treated with 10 μmol/L nutlin-3a or the same amount of DMSO for 24 h. After the treatment, ChIP was performed as described in Material and Methods. *B,* EMSA was carried out using biotinated oligonucleotides generated from the candidates of *p53* consensus DNA-binding sequence on the *ING2* regulatory regions, *ING* site 1 and site 2. Recombinant p53 protein and anti-p53 (DO-1) antibody were used for detecting shifted or super-shifted bands. Each unlabeled oligonucleotide (100-fold excess) was used as a competitor. *C,* four kinds of luciferase constructs using pGL-3 basic vector were designed as *A, B, C,* and *D*. Each 1.6 μg of a pGL-3 luciferase reporter and 0.16 μg of *Renilla* luciferase assay vector pRL were cotransfected into the p53 isogenic pairs of HCT116 and RKO cells. At 24 h later, 10 μmol/L nutlin-3a or the same amount of DMSO was added to cells for 12 h. Variation in transfection efficiency was normalized by *Renilla* luciferase activity. *Columns,* average of relative luciferase activity in three independent experiments; *bars,* SD.
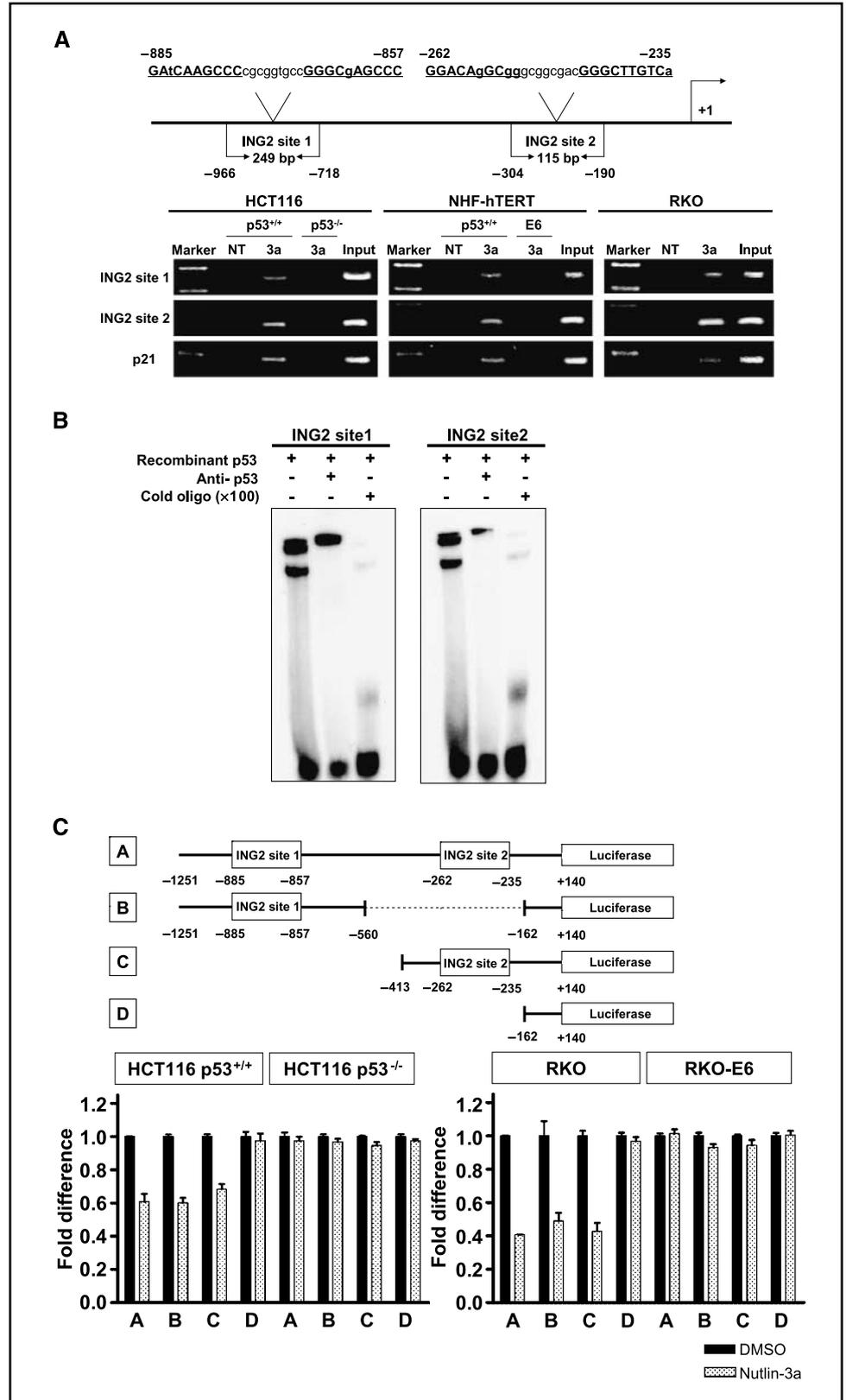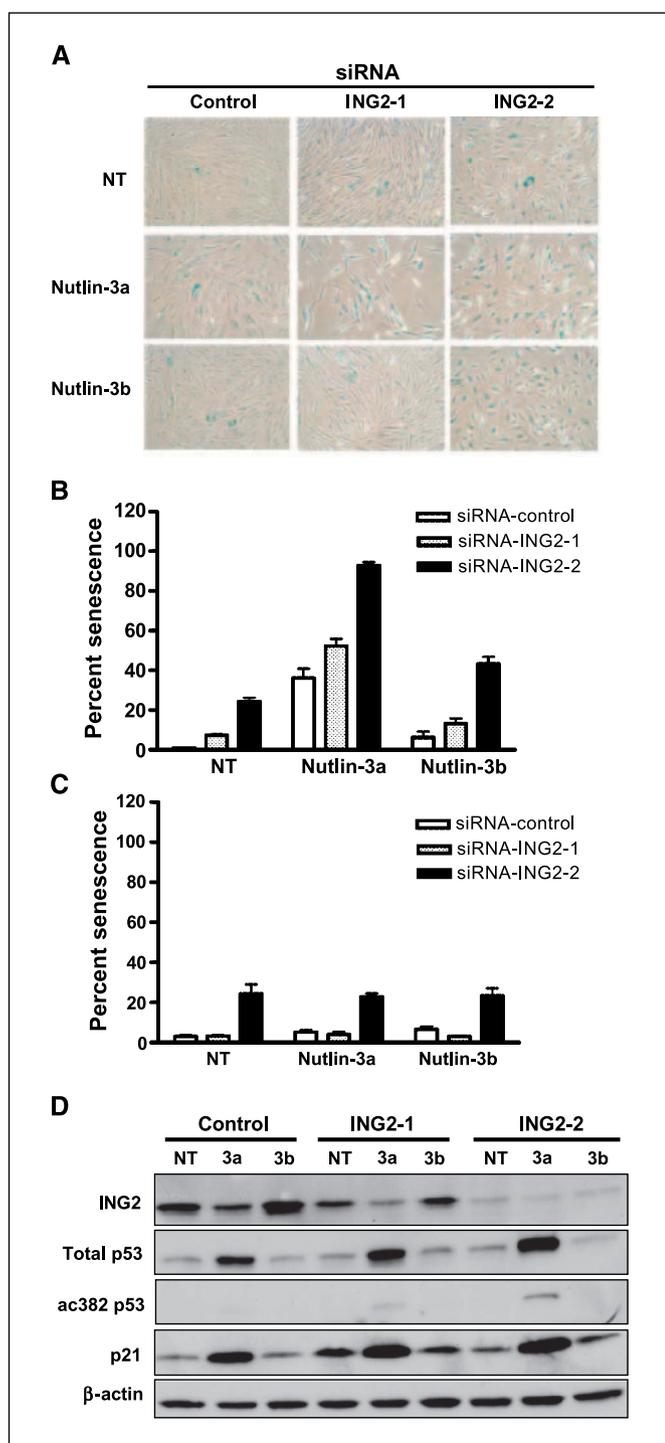
Figure 5. Down-regulation of ING2 induces cellular senescence. *A,* NHF-hTERT cells were treated with the following siRNA oligonucleotides at 100 nmol/L concentration: a random sequence control (control), an *ING2* siRNA which reduces ING2 levels by almost 50% (ING2-1), and an *ING-2* siRNA which almost completely inhibits ING2 expression (ING2-2) for 24 h. After the treatment, 10 μmol/L nutlin-3a or nutlin-3b was added to cells for 72 h. Cells were stained for SA-β-gal assay. Magnification, 200×. *B,* after the procedure as above, the percentage of blue-stained cells was calculated. *Columns,* five random fields were counted per dish in each experiment. Three separate experiments were done in triplicate, and the results were averaged. *Bars,* SD. *C,* 100 nmol/L siRNA ING2-2 or control was transfected to 041 p53$^{-/-}$ cells. 24 h later, cells were treated with 10 μmol/L nutlin-3a or nutlin-3b for 72 h. SA-β-gal assay was performed. The positive stained cells were counted and shown as percentage. *Columns,* same as above; *bars,* SD. *D,* protein lysates were made from cells treated as in *B* and immunoblotted with the indicated antibodies.

SA-β-gal staining. However, we did not observe any changes in both NHF-hTERT E6 and NHF-hTERT p53 shRNA cells when they were treated with nutlin-3a or nutlin-3b (Fig. 1*C*).

To verify the accumulation of p53 by nutlin-3a, Western blot analysis was performed. In NHF-hTERT cells, the total amount of p53 expression was increased by nutlin-3a, but not by nutlin-3b (Fig. 1*D*). Although phosphorylation was not seen on residue serine 15 of p53 in the nutlin-3a–treated cells in agreement with a previous report (16), acetylation of p53 residue 382 was present in the nutlin-3a–treated cells. p21 expression was also increased with nutlin-3a treatment. In contrast, there was no increase of p53 expression with nutlin-3a treatment in the p53 null cells. To confirm these observations, we examined p53 expression with nutlin-3 treatment using the p53 isogenic-paired cell lines, HCT116 p53$^{+/+}$ and HCT116 p53$^{-/-}$ cells. The result was very similar with the previous data from studies using human fibroblasts (Supplementary Fig. S3*A*).

According to a previous report, phosphorylation of threonine 18 is mediated by casein kinases (38), requiring the previous phosphorylation of serine 15, and this phosphorylation interferes with the p53 binding to MDM2 (39). Therefore, we examined the status of threonine 18 with nutlin-3 treatment. Phosphorylation on residue threonine 18 of p53 was not present in nutlin-3–treated NHF-hTERT cells (Supplementary Fig. S3*B*).

It has been reported that U-2OS, an osteosarcoma cell line which possesses a functional p53, did not exhibit the apoptotic phenotype after nutlin-3a (14). We hypothesized that nutlin-3a could induce senescence instead of apoptosis even in this cancer cell line. The levels of senescence were minimal at 7 days, but there was a significant increase seen at 14 days (Supplementary Fig. S4). According to the literature, the subset of apoptotic-associated genes regulated by p53 was lacking in U-2OS cells compared with cells that were strongly induced to undergo apoptosis by nutlin-3a treatment (14). The difference in cellular response by nutlin-3a can be explained from the defects downstream of p53.

Nutlin-3a–induced p53-responsive genes. The spectrum of p53-responsive genes differs depending on the types of stimuli (19). Therefore, we next examined the contribution of *p53* activation to gene expression after treatment with nutlin-3a using microarray technology. We compared the gene expression in NHF-hTERT and NHF-hTERT p53 shRNA cells with treatment of nutlin-3a or DMSO at 24 and 36 h using the univariate two-sample *t* test ($P < 0.05$) with randomized variance. A total of 2,942 genes were differentially expressed after nutlin-3a treatment, of which 1,737 genes (59%) were up-regulated and 1,205 genes (41%) were down-regulated (Supplementary Tables S1 and S2). Among the up-regulated genes, the expression of *BTG2, GDF15, TP53I3/PIG3, SULF2, NINJ1, PLTP,* and *SESN1* was strongly increased in a p53-dependent manner (Table 1). The well-known targets of *p53, BAX, GADD45A, TP53INP1, TP53AP1, CCNG1,* and *IGFBP3* were also detected as up-regulated genes. On the other hand, the expression of *CCNB1, CENPF, CCNA2, CDKN3, SPAG5, CKS2, CASC5, KIFC1, CDC20,* and *KIF2C* was remarkably decreased (Table 1). Additionally, the expression of minichromosome maintenance complex component (*MCM*) genes, including *MCM2* to *MCM8,* which are associated with DNA replication, and ING2, which is involved in chromatin remodeling and regulating gene expression, were down-regulated in NHF-hTERT cells treated with nutlin-3a.

p53 activates *mir-34* expression and suppresses ING2 expression. In addition to mRNA expression, recent reports have

shown that *mir-34a, mir-34b*, and *mir-34c* are regulated by p53 activation, suggesting that they have a potential function in the senescence pathway in normal human fibroblasts (24–27). We found that the expression of all three mir-34s were up-regulated by nutlin-3a treatment and that the response of *mir-34a* was earlier than *mir-34b* and *mir-34c* (Fig. 2A). *mir34a, mir34b*, and *mir34c* levels were shown to be up-regulated to varying amounts in various human tumor cell lines that were wild type for p53 after treatment with nutlin-3a after 24 hours (Fig. 2B–D). The tumor cell lines that were either p53 null or have a mutant p53 did not show this up-regulation.

We further focused on *ING2* as one of the *p53*-responsive genes from the microarray data because of previous studies of the *ING* family (28–32). We examined the ING2 expression when p53 was activated using nutlin-3a in NHF-hTERT cells. Interestingly, ING2 expression in the cells treated with nutlin-3a was remarkably decreased compared with nontreated cells while ING2 expression was not changed in nutlin-3b–treated cells (Fig. 3A).

To further show the association between p53 status and *ING2* expression, we examined other cell lines. p53 wild-type cells, including HCT116, RKO, LS174T, A549, MCF-7, and NHF-hTERT, were treated with 10 μmol/L of nutlin-3a or DMSO as a control. ING2 mRNA transcripts were consistently decreased by nutlin-3a treatment in all cell lines using a real-time PCR method, whereas *ING2* mRNA expression was not changed significantly in p53 mutant and null cells (Fig. 3B).

Next, we investigated whether the expression of *ING2* mRNA was altered in a dose-dependent and time-dependent manner by nutlin-3a treatment. In both HCT116 and RKO cells, the *ING2* mRNA level was down-regulated, depending on the dose, reaching a maximum level at 5 μmol/L at 24 h. Furthermore, the decrease in *ING2* expression was time dependent. *p21* mRNA expression was examined as a positive control of p53 activation and was up-regulated under the same conditions (Fig. 3C).

ING2 protein expression was examined using the p53 isogenic cell lines, HCT116 p53$^{+/+}$ and HCT116 p53$^{-/-}$, NHF-hTERT and NHF-hTERT p53 shRNA, to see whether the suppression occurs in a p53-dependent manner. The accumulation of p53 in HCT116 p53$^{+/+}$ was seen earlier than in NHF-hTERT (Fig. 3D). In p53 wild-type cells, ING2 protein expression was consistently decreased by the treatment with nutlin-3a in a p53-dependent manner. ING2 protein expression correlated with its mRNA expression level. There was no remarkable change in p53 null cells.

p53 binds to the ING2 promoter region and suppresses ING2 activity. We next analyzed the *ING2* promoter region for a p53-DNA consensus binding sequence by computational analysis.[7] Two regions that were strongly suspected as candidates were detected on the *ING2* regulatory region within 1.5 kb. The regions between −885 and −857 (ING2 site 1) and −262 and −235 (ING2 site 2) contain two motifs that closely resemble the PuPuPuCA/TA/TGPyPyPy consensus binding site for p53 (Fig. 4A).

To examine if wild-type p53 binds to the *ING2* promoter, we first performed ChIP assays. The primer pairs were constructed to detect each sequence for *ING2*, site 1 and site 2. As a positive control, the p53-DNA consensus binding sequence on the *p21* promoter region was also examined. Cells were left untreated or treated with nutlin-3a for 24 h. Lysates were

harvested and cross-linked, and then immunoprecipitations were performed using an antibody directed against p53. Promoter fragments of *ING2* site 1, site 2, and p21 were amplified by PCR and a representative agarose gel of the PCR products is shown in Fig. 4A. The PCR bands were detected at both sites 1 and 2 under treatment with nutlin-3a in p53 wild-type cells, whereas no bands were detected in the control cells and p53 null cells.

The EMSA was performed using biotinylated double-stranded oligonucleotides corresponding to the sequence of *ING2* sites 1 and 2. Recombinant p53 protein was used for these experiments. The shifted bands were detected in both *ING2* sites 1 and 2 (Fig. 4B). An antibody to p53 generated a super-shifted complex for both sites 1 and 2 of *ING2*, further confirming that the binding is specific. Moreover, when the unlabeled double-stranded oligonucleotides corresponding to *ING2* sites 1 and 2 were used as competitors, the formation of complexes was inhibited in each case, supporting the specificity of the DNA-p53 complex for these putative sites.

To determine whether the decrease in *ING2* mRNA is dependent on the function of p53 as a regulator of transcription, we analyzed the regulation of the *ING2* promoter. For this purpose, four kinds of constructs were generated and cloned into the pGL3 luciferase vector. The longest construct (A) from −1251 to +140 included both *ING2* site 1 and site 2. The construct (B) lacked the site 2, and the construct (C) had only the site 2. The construct (D) was deleted of both sites 1 and 2 as a negative control. These constructs were transiently cotransfected with *Renilla* luciferase vector into the p53 isogenic pairs of HCT116 and RKO cell lines. After transfection, the cells were treated with nutlin-3a for 12 hours. In p53 wild-type cells, the luciferase activity in nutlin-3a–treated cells was clearly down-regulated in the constructs (A), (B), and (C) of the *ING2* promoter when compared with the nontreated cells, whereas there was no remarkable change in the construct (D) between nutlin-3a–treated and nontreated cells (Fig. 4C). No significant alteration of the luciferase activity was detected in nutlin-3a–treated and nontreated p53 deficient cells (Fig. 4C).

Both *ING2* site 1 and site 2 share similar sequences with the Sp1 consensus sequence (Supplementary Fig. S5A). Previous reports showed Sp1 was involved in the repression mechanism by p53 (40–43). To investigate whether Sp1 can bind to these sites, EMSA was performed using recombinant Sp1 protein. The labeled oligonucleotides of a typical Sp1 consensus sequence were used as a positive control. A shifted band was detected at *ING2* site 2, but not detected at site 1 (Supplementary Fig. S5A). Moreover, we examined the binding affinity at *ING2* site 2 with the competition of Sp1 and p53. When both Sp1 and p53 were added, p53 dominantly bound to ING2 site 2 (Supplementary Fig. S5B). It has previously been shown that negative regulation of transcription by p53 may involve p53-mediated recruitment of HDAC and mSin3A (44); therefore, we tested whether this is also true for the *ING2* promoter. HCT116 cells were treated with trichostatin A to inhibit HDAC activity. ING2 expression was not attenuated by a combined treatment with nutlin-3a and trichostatin A (Supplementary Fig. S5C). In the luciferase assay, the activity was not repressed by the same treatment (Supplementary Fig. S5D).

Disregulation of ING2 induces senescence. We have previously shown that overexpression of ING2 can induce p53-dependent senescence (45). We have confirmed this result (Supplementary Fig. S6). We also have shown that down-regulation of ING2 by siRNA

---

[7] http://bioinformatics.med.ohio-state.edu/P53/

technology induces cellular senescence (Fig. 5*A* and *B*) that is p53 independent (Fig. 5*C* and *D*).

Discussion

We found that nutlin-3a induced senescence in normal human fibroblasts in a time-dependent, dose-dependent, and p53-dependent manner. A complimentary report showed that nutlin-3a induces cellular senescence in murine fibroblasts in a p53-dependent manner (46). Although phosphorylation was not seen on residue serine 15 of p53 after nutlin-3a treatment, acetylation of p53 residue 382 was detected. Previous studies have implicated ING1 and 2 in acetylation of p53 at lysine 382 (46, 47) and acetylation of p53 K382 increases during cell senescence (3). In addition, we examined the phosphorylation status at threonine 18 with nutlin-3 treatment, because this modification was previously found to be associated with MDM2 (39). Although we could not detect this p53 phosphorylation with nutlin-3 treatment, unlike doxorubicin treatment, p53 could still function as a transcriptional factor because *p21* and *mir-34a, mir-34b*, and *mir-34c* expression was increased. It has been reported that the phosphorylation on the NH_2 terminal of p53 was not required for p53-dependent transcription based on the result that ARF-induced p53 was not phosphorylated on the NH_2 terminal of p53, including serine 6, 9, 15, 20, and 37, but showed the phosphorylation at serine 392 (48). Therefore, phosphorylation on the NH_2 terminal of p53 seems not be essential for induction of p53-dependent senescence.

Previously, we reported that p53 activation by treatment with several stimuli regulated various genes positively and negatively depending on the stimuli (19). To better understand the association with nutlin-3a–induced p53 and senescence in human fibroblasts, microarray experiments were performed. We found that the genes up-regulated by nutlin-3a treatment were associated with antiproliferative and proapoptotic functions. Plasminogen activator inhibitor-1 was one of these genes and is a potential p53 target and involved in cellular senescence (3, 49). As to the down-regulated genes, cell cycle and DNA replication-related genes, such as *CCNB1, CCNB2, CCNA2, CKN3*, and *MCM* family genes, were significantly decreased.

According to recent reports, *mir-34a, mir-34b*, and *mir-34c*, which are induced by p53 activation, are downstream effectors of p53 (24–27). Overexpression of *mir-34a, mir-34b*, and *mir-34c* has been shown to induce senescence in normal human fibroblasts (24). We confirmed that all three of the mir-34s were increased in nutlin-3a–treated NHF-hTERT cells. Whereas *mir-34a, mir-34b*, and *mir-34c* were not induced by nutlin-3a in the p53 null or mutant cell lines, the level of induction varied among the cancer cell lines with wild-type p53. These data support the hypothesis that *mir-34a, mir-34b*, and *mir-34c* are involved in the p53-dependent senescence pathway.

We found that *ING2* mRNA transcripts were suppressed by nutlin-induced p53 activation from the microarray data. We also detected a decrease of ING2 protein expression in nutlin-3a–treated cells and *ING2* mRNA levels were consistently down-regulated with nutlin-3a treatment in p53 wild-type cells, whereas there was no remarkable change in p53-mutant and p53-deficient cells. Recently, there is evidence that a large number of genes are suppressed by p53 (19–21). It has been reported that p53 consensus DNA-binding sequences have been found among genes repressed in a p53-dependent manner (20, 21). Recent reports have indicated that some of these down-regulated genes

might be associated with microRNA expression. In fact, *mir-34a* was determined to regulate a subset of p53 related genes (24). We investigated whether overexpression of *mir-34a* could regulate *ING2* expression. *ING2* expression in *mir-34a* overexpressed cells was not altered (Supplementary Fig. S7).

We found candidates of p53 consensus DNA-binding sequences on the *ING2* regulatory region within 1.5 kb and confirmed the p53 binding ability to the expected sites from ChIP assay and EMSA. Furthermore, the data from the luciferase assays showed p53 could repress *ING2* promoter activity. There was sufficient evidence that p53 repressed *ING2* and this phenomenon might be occurring through p53 binding directly to the consensus DNA-binding sequences on the *ING2* regulatory region. At least, three kinds of mechanisms have been proposed (51). First, p53 may interact with DNA-binding transcriptional activators and interfering with the function of activators. This mechanism includes the competition between p53 and activators through the overlapping DNA binding site. Second, p53 may interact with components of the basal transcriptional machinery. Finally, p53 may recruit chromatin modifying factors, such as HDAC, so that gene expression could be suppressed. These three mechanisms of p53 transcriptional repression can also act in combination (40). Based on these previous studies, we first investigated the possibility that other transcriptional factors could bind to the p53 consensus DNA-binding sequences on the *ING2* promoter. Both ING2 sites 1 and 2 share similar sequences with the Sp1 consensus sequence. One of the mechanisms of *ING2* suppression by p53 could be explained that p53 binding affinity to the promoter region was stronger than Sp1, which might regulate *ING2* expression endogenously.

Recent reports indicate that ING2 has the ability to bind the histone H3 trimethylated at lysine 4 (31–33). Consequently, ING2 is involved in chromatin remodeling to regulate gene activation or suppression. Chromatin structure consists of many forms of modification that drastically regulate gene transcription; thus, the impairment of these epigenetic events may affect tumor development, cell proliferation, and senescence (36). A previous report shows ING2 suppresses *cyclin D1* mRNA expression in response to DNA damage (32). It is well known that cyclin D1 has diverse effects on cells depending on its level of expression and cell type (51). For example, *cyclin D1* expression is increased in senescent cells compared with young cells (52, 53). Based on this evidence, there is the possibility that the down-regulation of ING2 results in the enhancement of cyclin D1 to modulate senescence.

In addition to the induction of senescence by down-regulation of ING2, overexpression of ING2 can also induce senescence. The senescence induced by knockdown of ING2 is p53 independent, whereas the senescence induced by overexpression of ING2 is p53 dependent. These results suggest that both different mechanisms and the physiologic range of ING2 levels may be important to maintain cellular homeostasis. Further studies with either ING2 transgenic or knockout mice will be interesting to pursue.

Acknowledgments

References

1. Vousden KH, Lane DP. p53 in health and disease. Nat Rev Mol Cell Biol 2007;8:275–83.
2. Itahana K, Dimri G, Campisi J. Regulation of cellular senescence by p53. Eur J Biochem 2001;268:2784–91.
3. Serrano M, Lin AW, McCurrach ME, Beach D, Lowe SW. Oncogenic ras provokes premature cell senescence associated with accumulation of p53 and p16INK4a. Cell 1997;88:593–602.
4. Hayflick L, Moorhead PS. The limited *in vitro* lifetime of human diploid cell strains. Exp Cell Res 1961;25:585–621.
5. Collado M, Gil J, Efeyan A, et al. Tumour biology: senescence in premalignant tumours. Nature 2005; 436:642.
6. Braig M, Schmitt CA. Oncogene-induced senescence: putting the brakes on tumor development. Cancer Res 2006;66:2881–4.
7. Haupt Y, Maya R, Kazaz A, Oren M. Mdm2 promotes the rapid degradation of p53. Nature 1997;387:296–9.
8. Oliner JD, Kinzler KW, Meltzer PS, George DL, Vogelstein B. Amplification of a gene encoding a p53-associated protein in human sarcomas. Nature 1992; 358:80–3.
9. Pomerantz J, Schreiber-Agus N, Liegeois NJ, et al. The Ink4a tumor suppressor gene product, p19Arf, interacts with MDM2 and neutralizes MDM2's inhibition of p53. Cell 1998;92:713–23.
10. Zhang Y, Xiong Y, Yarbrough WG. ARF promotes MDM2 degradation and stabilizes p53: ARF-INK4a locus deletion impairs both the Rb and p53 tumor suppression pathways. Cell 1998;92:725–34.
11. Vassilev LT. MDM2 inhibitors for cancer therapy. Trends Mol Med 2007;13:23–31.
12. Vassilev LT. p53 Activation by small molecules: application in oncology. J Med Chem 2005;48:4491–9.
13. Vassilev LT, Vu BT, Graves B, et al. *In vivo* activation of the p53 pathway by small-molecule antagonists of MDM2. Science 2004;303:844–8.
14. Tovar C, Rosinski J, Filipovic Z, et al. Small-molecule MDM2 antagonists reveal aberrant p53 signaling in cancer: implications for therapy. Proc Natl Acad Sci U S A 2006;103:1888–93.
15. Coll-Mulet L, Iglesias-Serret D, Santidrian AF, et al. MDM2 antagonists activate p53 and synergize with genotoxic drugs in B-cell chronic lymphocytic leukemia cells. Blood 2006;107:4109–14.
16. Thompson T, Tovar C, Yang H, et al. Phosphorylation of p53 on key serines is dispensable for transcriptional activation and apoptosis. J Biol Chem 2004;279:53015–22.
17. LaRusch GA, Jackson MW, Dunbar JD, Warren RS, Donner DB, Mayo LD. Nutlin3 blocks vascular endothelial growth factor induction by preventing the interaction between hypoxia inducible factor 1α and Hdm2. Cancer Res 2007;67:450–4.
18. Ambrosini G, Sambol EB, Carvajal D, Vassilev LT, Singer S, Schwartz GK. Mouse double minute antagonist nutlin-3a enhances chemotherapy-induced apoptosis in cancer cells with mutant p53 by activating E2F1. Oncogene 2007;26:3473–81.
19. Staib F, Robles AI, Varticovski L, et al. The p53 tumor suppressor network is a key responder to microenvironmental components of chronic inflammatory stress. Cancer Res 2005;65:10255–64.
20. Robinson M, Jiang P, Cui J, et al. Global genechip profiling to identify genes responsive to p53-induced growth arrest and apoptosis in human lung carcinoma cells. Cancer Biol Ther 2003;2:406–15.
21. Mirza A, Wu Q, Wang L, et al. Global transcriptional program of p53 target genes during the process of apoptosis and cell cycle progression. Oncogene 2003;2:3645–54.
22. Shelton DN, Chang E, Whittier PS, Choi D, Funk WD. Microarray analysis of replicative senescence. Curr Biol 1999;9:939–45.
23. Komarova EA, Diatchenko L, Rokhlin OW, et al. Stress-induced secretion of growth inhibitors: a novel tumor suppressor function of p53. Oncogene 1998;17:1089–96.
24. He L, He X, Lim LP, et al. A microRNA component of the p53 tumour suppressor network. Nature 2007;447:1130–4.
25. Raver-Shapira N, Marciano E, Meiri E, et al. Transcriptional activation of miR-34a contributes to p53-mediated apoptosis. Mol Cell 2007;26:731–43.
26. Chang TC, Wentzel EA, Kent OA, et al. Transactivation of miR-34a by p53 broadly influences gene expression and promotes apoptosis. Mol Cell 2007;26:745–52.
27. Tarasov V, Jung P, Verdoodt B, et al. Differential regulation of microRNAs by p53 revealed by massively parallel sequencing: miR-34a is a p53 target that induces apoptosis and G(1)-arrest. Cell Cycle 2007;6:1586–93.
28. He GH, Helbing CC, Wagner MJ, Sensen CW, Riabowol K. Phylogenetic analysis of the ING family of PHD finger proteins. Mol Biol Evol 2005;22:104–16.
29. Nagashima M, Shiseki M, Miura K, et al. DNA damage-inducible gene p33ING2 negatively regulates cell proliferation through acetylation of p53. Proc Natl Acad Sci U S A 2001;98:9671–6.
30. Doyon Y, Cayrou C, Ullah M, et al. ING tumor suppressor proteins are critical regulators of chromatin acetylation required for genome expression and perpetuation. Mol Cell 2006;21:51–64.
31. Pena PV, Davrazou F, Shi X, et al. Molecular mechanism of histone H3K4me3 recognition by plant homeodomain of ING2. Nature 2006;442:100–3.
32. Shi X, Hong T, Walter KL, et al. ING2 PHD domain links histone H3 lysine 4 methylation to active gene repression. Nature 2006;442:96–9.
33. Ruthenburg AJ, Allis CD, Wysocka J. Methylation of lysine 4 on histone H3: intricacy of writing and reading a single epigenetic mark. Mol Cell 2007;25:15–30.
34. Santos-Rosa H, Schneider R, Bannister AJ, et al. Active genes are tri-methylated at K4 of histone H3. Nature 2002;419:407–11.
35. Bernstein BE, Kamal M, Lindblad-Toh K, et al. Genomic maps and comparative analysis of histone modifications in human and mouse. Cell 2005;120:169–81.
36. Han X, Berardi P, Riabowol K. Chromatin modification and senescence: linkage by tumor suppressors? Rejuvenation Res 2006;9:69–76.
37. Dimri GP, Lee X, Basile G, et al. A biomarker that identifies senescent human cells in culture and in aging skin *in vivo*. Proc Natl Acad Sci U S A 1995;92:9363–7.
38. Sakaguchi K, Saito S, Higashimoto Y, Roy S, Anderson CW, Appella E. Damage-mediated phosphorylation of human p53 threonine 18 through a cascade mediated by a casein 1-like kinase. Effect on Mdm2 binding. J Biol Chem 2000;275:9278–83.
39. Craig AL, Burch L, Vojtesek B, Mikutowska J, Thompson A, Hupp TR. Novel phosphorylation sites of human tumour suppressor protein p53 at Ser20 and Thr18 that disrupt the binding of mdm2 (mouse double minute 2) protein are modified in human cancers. Biochem J 1999;342:133–41.
40. Sengupta S, Shimamoto A, Koshiji M, et al. Tumor suppressor p53 represses transcription of RECQ4 helicase. Oncogene 2005;24:1738–48.
41. Kanaya T, Kyo S, Hamada K, et al. Adenoviral expression of p53 represses telomerase activity through down-regulation of human telomerase reverse transcriptase transcription. Clin Cancer Res 2000;6:1239–47.
42. Ohlsson C, Kley N, Werner H, LeRoith D. p53 regulates insulin-like growth factor-I (IGF-I) receptor expression and IGF-I-induced tyrosine phosphorylation in an osteosarcoma cell line: interaction between p53 and Sp1. Endocrinology 1998;139:1101–7.
43. Li B, Lee MY. Transcriptional regulation of the human DNA polymerase δ catalytic subunit gene POLD1 by p53 tumor suppressor and Sp1. J Biol Chem 2001;276:29729–39.
44. Murphy M, Ahn J, Walker KK, et al. Transcriptional repression by wild-type p53 utilizes histone deacetylases, mediated by interaction with mSin3a. Genes Dev 1999;13:2490–501.
45. Pedeux R, Sengupta S, Shen JC, et al. ING2 regulates the onset of replicative senescence by induction of p300-dependent p53 acetylation. Mol Cell Biol 2005;25:6639–48.
46. Efeyan A, Ortega-Molina A, Velasco-Miguel S, Herranz D, Vassilev LT, Serrano M. Induction of p53-dependent senescence by the MDM2 antagonist nutlin-3a in mouse cells of fibroblast origin. Cancer Res 2007;67:7350–7.
47. Kataoka H, Bonnefin P, Vieyra D, et al. ING1 represses transcription by direct DNA binding and through effects on p53. Cancer Res 2003;63:5785–92.
48. Jackson MW, Agarwal MK, Agarwal ML, et al. Limited role of N-terminal phosphoserine residues in the activation of transcription by p53. Oncogene 2004;23:4477–87.
49. Kortlever RM, Higgins PJ, Bernards R. Plasminogen activator inhibitor-1 is a critical downstream target of p53 in the induction of replicative senescence. Nat Cell Biol 2006;8:877–84.
50. Ho J, Benchimol S. Transcriptional repression mediated by the p53 tumour suppressor. Cell Death Differ 2003;10:404–8.
51. Han EK, Ng SC, Arber N, Begemann M, Weinstein IB. Roles of cyclin D1 and related genes in growth inhibition, senescence and apoptosis. Apoptosis 1999;4:213–9.
52. Fukami J, Anno K, Ueda K, Takahashi T, Ide T. Enhanced expression of cyclin D1 in senescent human fibroblasts. Mech Ageing Dev 1995;81:139–57.
53. Atadja P, Wong H, Veillete C, Riabowol K. Overexpression of cyclin D1 blocks proliferation of normal diploid fibroblasts. Exp Cell Res 1995;217:205–16.

Nutlin-3a Activates p53 to Both Down-regulate Inhibitor of Growth 2 and Up-regulate *mir-34a, mir-34b,* and *mir-34c* Expression, and Induce Senescence

Kensuke Kumamoto, Elisa A. Spillare, Kaori Fujita, et al.

Updated version	Access the most recent version of this article at: http://cancerres.aacrjournals.org/content/68/9/3193
Supplementary Material	Access the most recent supplemental material at: http://cancerres.aacrjournals.org/content/suppl/2008/04/25/68.9.3193.DC1

Cited articles	This article cites 53 articles, 17 of which you can access for free at: http://cancerres.aacrjournals.org/content/68/9/3193.full#ref-list-1
Citing articles	This article has been cited by 23 HighWire-hosted articles. Access the articles at: http://cancerres.aacrjournals.org/content/68/9/3193.full#related-urls

E-mail alerts	Sign up to receive free email-alerts related to this article or journal.
Reprints and Subscriptions	To order reprints of this article or to subscribe to the journal, contact the AACR Publications Department at pubs@aacr.org.
Permissions	To request permission to re-use all or part of this article, use this link http://cancerres.aacrjournals.org/content/68/9/3193. Click on "Request Permissions" which will take you to the Copyright Clearance Center's (CCC) Rightslink site.